Semiconductor Raman Amplifier for Terahertz Bandwidth Optical Communication

Ken Suto, *Member, IEEE*, Takao Saito, *Member, IEEE*, Tomoyuki Kimura, Jun-Ichi Nishizawa, *Life Fellow, IEEE*, and Tadao Tanabe

***Abstract*—Semiconductor Raman amplifiers are useful for frequency selection in terahertz bandwidth and wavelength division multiplexing (WDM) systems with terabit capacity, as well as direct terabit optical communication systems. We have developed GaP–AlGaP Raman waveguides with micrometer-size cross sections. We have reduced residual optical loss of the waveguide by improvement of the fabrication process and realized a low-loss waveguide that is 10-mm long, which has a continuous wave (CW) Raman gain of 3.7 dB. Also, the time-gated amplification with 80-ps pulse pumping is performed and 20-dB gain is obtained. These performances are very suitable for light frequency selection in terahertz bandwidth and WDM optical communication systems.**

***Index Terms*—GaP, Raman amplifier, Raman laser, semiconductor waveguide, terabit, terahertz bandwidth, wavelength division multiplexing (WDM).**

I. Introduction

SEMICONDUCTOR Raman lasers and amplifiers are promising devices for light frequency selection in terahertz bandwidth optical communications as well as wavelength division multiplexing (WDM) optical communications with terabit-per-second capacity.

After the first proposal of the semiconductor Raman lasers for use in optical communication [1], Raman oscillation in semiconductors was first realized in GaP single crystals [2]. It is noted that spontaneous Raman scattering in GaP was extensively studied [3], [4]. Also, it is noted that there are fiber Raman lasers [5] and $LiNbO_3$ Raman lasers [6] useful in optical communication. The semiconductor waveguide Raman lasers and amplifiers with a GaP core layer and AlGaP cladding layers were developed, which drastically decreased the threshold pump power [7]. The lowest threshold pump power of the Raman laser was as low as 50 mW [8], and pumping by a laser diode with single longitudinal mode was realized [9]. It was shown that the intensity noise of the Raman laser is reduced 30 dB below that of the pump source [10]. This is a very useful feature of the semiconductor Raman laser. The mechanism of noise reduction was shown to be the transmission of the noise power of the pump light to the second Stokes light, which stabilizes the first Stokes light power.

At the same time, the Raman amplifier was shown to be effective for light frequency selection [11].This function will be useful in terahertz bandwidth optical communication systems as well as in WDM systems with terabit-per-second capacity. The selection of a signal light with frequency ω_s is made by tuning the pump light frequency ω_p to satisfy the relationship $\omega_p = \omega_{ph} + \omega_s$ where ω_{ph} is the longitudinal optical phonon frequency and ω_s corresponds to the Stokes light frequency, which is to be amplified.

In the case of GaP, the crystallographic direction of the waveguide is $\langle 100 \rangle$, for which stimulated Raman scattering from the longitudinal optical (LO) phonons with a frequency of 12.12 THz takes place dominantly in the backward direction. The LO phonon Raman scattering in the forward direction has been shown to be very weak in a waveguide having a cross section with micrometer size. This is due to the large wave momentum components in the transverse directions in a narrow waveguide [12], [13].

The full-width at half-maximum (FWHM) of the Raman gain coefficient was measured to be 23.5 GHz. This fact means that we can discriminate about 40 frequency channels within a light frequency bandwidth of 1 THz. In our recent paper, it has been shown that the Raman gain coefficient of GaP is $g = 12.3 \times 10^{-8}$ Wcm^{-1} [12]. This value is about five times that of CS_2 and $LiNbO_3$, which were estimated to have the highest Raman gain coefficients. In our experiment, the highest Raman gain with continuous wave pumping in a 10-mm-long GaP–AlGaP waveguide has been 2.57 dB, which is smaller than the Raman gain expected from the results in shorter waveguides. The most important element that limits the amplifier gain is the optical loss caused by various kinds of imperfections in the waveguide. This paper reports on the improvement of the waveguide perfection and the increase of CW-pumped Raman gain. Also, we provide the experimental results of pumping by pulsed laser light. Pulse pumping enables the time gate function necessary for pulse channel selection simultaneously with the wavelength selection. The pulse pumping has another benefit that much higher Raman gain is easily obtained. On the basis of these results, we discuss the estimation of available highest gain in relation to the waveguide structure, and capability of the semiconductor Raman amplifier for channel selection in wide-band optical communication systems.

Manuscript received May 16, 2001; revised December 17, 2001.

K. Suto is with the Department of Materials Science, Tohoku University, Sendai 980-0862, Japan, and also with the Telecommunication Advancements Organization, Sendai Research Center, Sendai 980-0862, Japan.

T. Saito and T. Tanabe are with the Department of Materials Science, Tohoku University, Sendai 980-0862, Japan.

T. Kimura is with the Telecommunication Advancements Organization, Sendai Research Center, Sendai 980-0862, Japan.

J.-I. Nishizawa is with the Telecommunication Advancements Organization, Sendai Research Center, Sendai 980-0862, Japan, and also with the Semiconductor Research Institute, Sendai 980-0862, Japan.

Publisher Item Identifier S 0733-8724(02)02854-2.

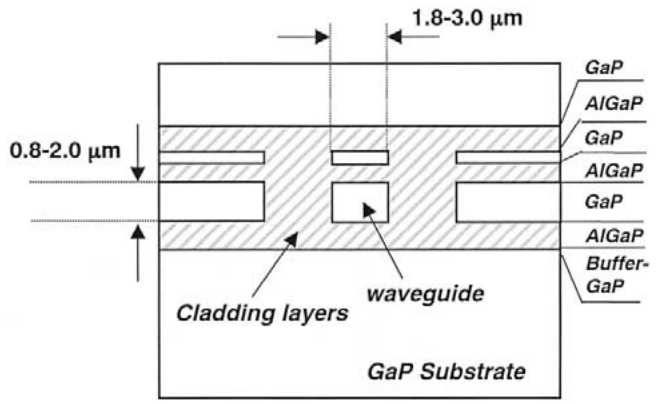

Fig. 1. Illustration of the cross-sectional view of a Raman amplifier waveguide.

II. Device Structure and Fabrication

Fig. 1 illustrates the structure of the semiconductor Raman amplifier. The waveguide is formed in the $\langle 100 \rangle$ direction on a GaP substrate with the $\langle 001 \rangle$ surface. The core of the waveguide is made of a GaP epitaxial layer and the cladding layers are made of $Al_xGa_{1-x}P$ epitaxial layers. The thickness d and the width w of the core are in the range 0.8 to 2.0 μm, and 1.8 to 3 μm, respectively, and the length l of the waveguide is 5 to 10 mm. The refractive index of $Al_xGa_{1-x}P$ is given by $n = 3.218 - 0.343x$ at a wavelength near 1 μm. With proper selection and the Al composition x in the range of 0.05 to 0.15, sufficient optical confinement in the core region can be obtained. Although higher modes can propagate in the waveguide, only the fundamental modes are actually excited for both the pump and signal. The input facet of the waveguide is antireflection (AR) coated, whereas the facet at the back end is high-reflection coated with $R = 98\%$. Both the pump light and the signal light introduced from the AR-coated front facet are reflected back at the back facet and taken out from the front facet. The stimulated LO phonon Raman scattering takes place mainly in the backward direction in the waveguide.

The fabrication processes are illustrated in Fig. 2. First, five layers of GaP–$Al_xGa_{1-x}P$–GaP–$Al_xGa_{1-x}P$–GaP are grown with the temperature difference method under controlled vapor pressure (TDM-CVP) liquid phase epitaxy (LPE) [14], [15]. The first GaP layer is a buffer layer for smooth growth of the first $Al_xGa_{1-x}P$ cladding layer, the second GaP layer is a core layer, and the third GaP layer is a buffer layer for the following regrowth process.

The next process is to form the stripes with photolithography and reactive ion etching (RIE) using Cl_2+Ar or PCl_3 gases.

The third process is to regrow two over layers of $Al_xGa_{1-x}P$–GaP. Finally, the input facet and the back facet of a waveguide are coated with an AR film and a 98% reflection film made of SiO_2 and TiO_2 multilayers, respectively.

Fig. 3 illustrates the experimental system for CW-pumped Raman amplification. The pump light beam from a TI–sapphire ring laser is introduced to the input facet of the Raman amplifier via an optical isolator and a cubic polarizer. The pump light wavelength is set at 824 nm. The signal light beam from a distributed Bragg reflector (DBR) laser diode with a wavelength

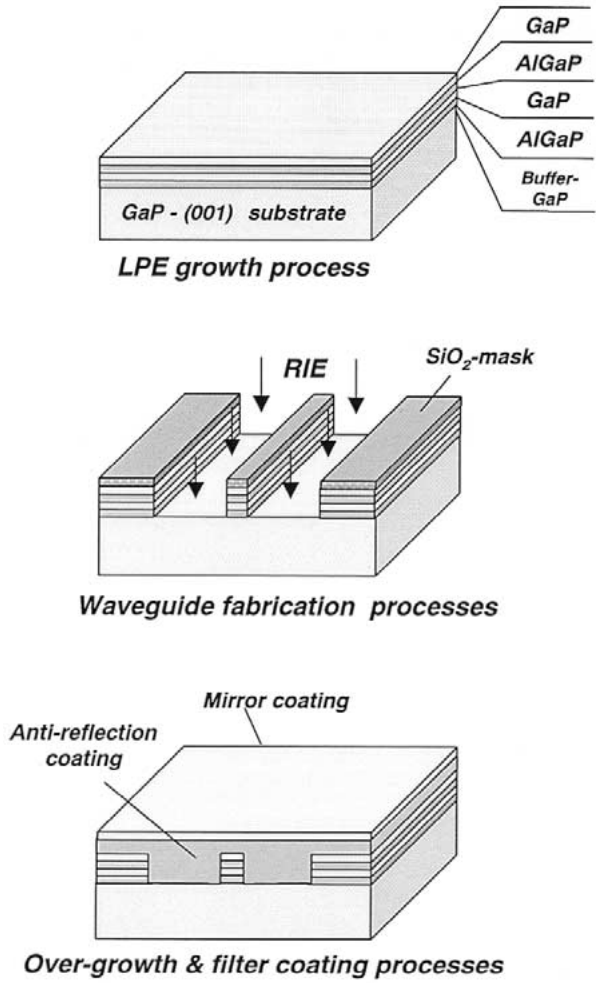

Fig. 2. Fabrication process of the Raman amplifier waveguide.

of 853 nm is also introduced to the input facet of the Raman amplifier via two optical isolators and the cubic polarizer. The amplified signal light from the Raman amplifier taken out from the front facet is introduced to a monochromator via the cubic polarizer and one of the optical isolators. The output beam from the monochromator is fed to a p-i-n photodiode. The DBR laser diode frequency can be continuously swept over 300 GHz by changing the diode temperature with a Peltier controller. There is no instability of the laser diode output power and the lasing frequency during the frequency sweep operation.

Pulse-pumping experiments have also been performed using a similar optical system. A mode-locked Ti sapphire laser is used as a pump light source. The pump pulsewidth and repetition frequency are 80 ps and 80 MHz, respectively. A frequency tunable continuous wave laser diode is used as a signal light source. The pump and signal light wavelengths are set at 925 and 960 nm, respectively. The photodiode in this system has a detection bandwidth of 25 GHz.

III. Characteristics of the Semiconductor Raman Amplifier

The main optical loss in a bulk GaP is the free carrier absorption. The free carrier absorption coefficient was measured to be

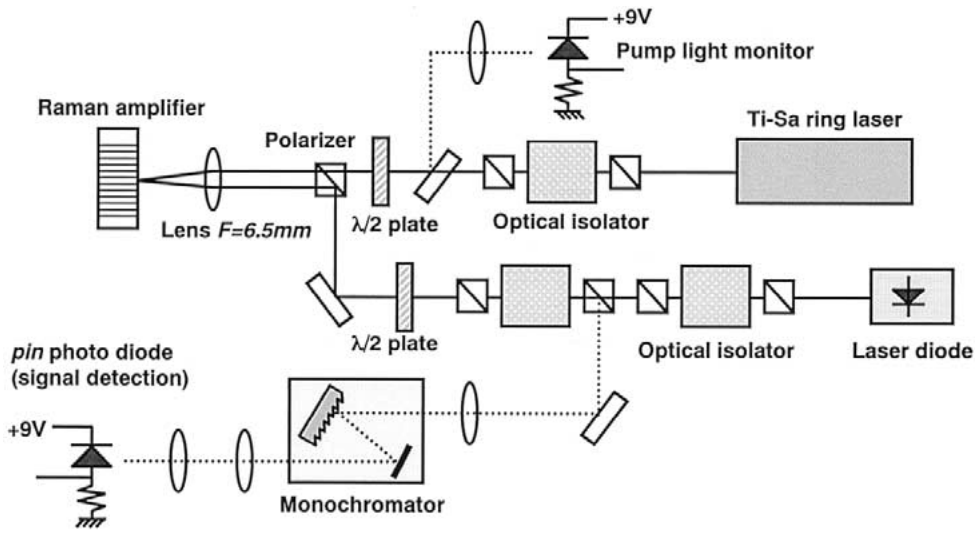

Fig. 3. Experimental setup for the Raman gain measurement.

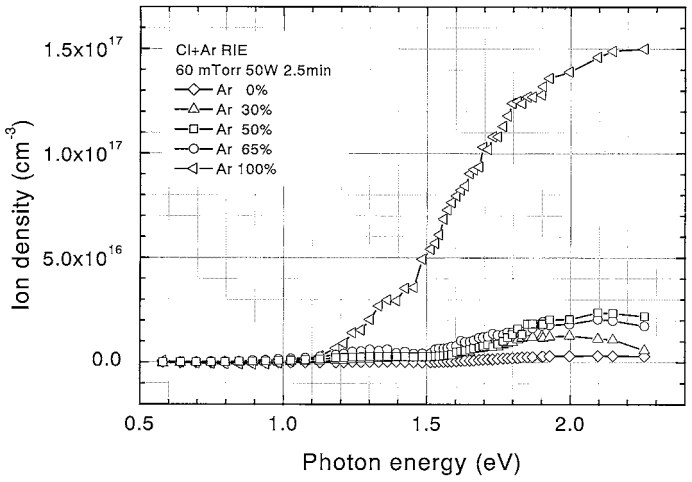

Fig. 4. Photocapacitance spectra of RIE-treated GaP for different ratios of Ar–Cl_2.

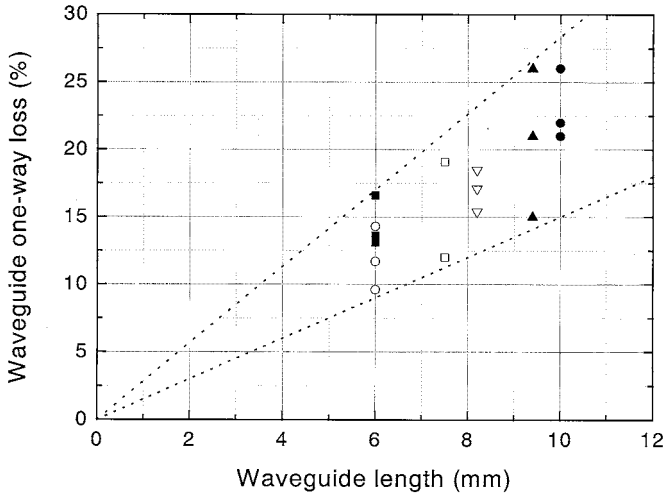

Fig. 5. Minimum optical losses of various Raman waveguides with different lengths.

given by $\alpha = 0.05\ \text{cm}^{-1} N/10^{16}\ \text{cm}^{-3}$, where N is the free carrier concentration. For the LPE using TDM-CVP method, we can obtain $N < 5 \times 10^{15}\ \text{cm}^{-3}$, which corresponds to $\alpha < 0.025\ \text{cm}^{-1}$. However, the waveguide optical loss estimated from the measurement of the finesse of a waveguide is usually much larger. There are three important sources of the excess optical loss, which prevent the high gain operation of long waveguides. One is the increase of the free carrier concentration at the regrowth interfaces. It was made clear that the increase is due to the contamination by silicon impurities. Among different acids for etching solutions, HCl solution has been the best for the reduction of the silicon contamination [16].

The second source of the optical loss is the formation of deep levels caused by the RIE process. Fig. 4 shows the photocapacitance spectrum of the RIE-treated GaP with different ratio of Ar–Cl_2, details of which will be described elsewhere. Although the deep level density decreases with decreasing Ar concentration, Ar is necessary for directional etching so that we have used the Ar–Cl_2 ratio of 1.8. A secondary ion mass spectrometry (SIMS) measurement has shown that the Cl ion is penetrated to a depth of about 60 to 100 nm from the surface in the RIE process. Therefore, the RIE-etched surface has been etched with H_2SO_4 to remove the damaged layer and then rightly etched by HCl solution to decrease Si contamination.

The third source is the diffusion of nonstoichiometric point defects from the substrate GaP single crystals to the epitaxial layer causing considerable increase of deep level density in the GaP core layer. The growth of the buffer layer of GaP on the substrate crystal is effective for the decrease in the deep level density. Also, the heat treatment of a substrate crystal at 900 °C to 850 °C causes an order-of-magnitude decrease in the nonstoichiometric deep levels in the substrate crystal [17].

The actual optical losses can be obtained by the measurement of the finesses of waveguides [12]. In this measurement, the front and back facets of a waveguide are uncoated and the resonance due to the reflections at both facets are measured by sweeping the signal light frequency via change of the DBR laser diode temperature. Fig. 5 shows the measured minimum optical losses for various lengths of the waveguides. It is seen that the minimum one-way loss with the improved device processes is

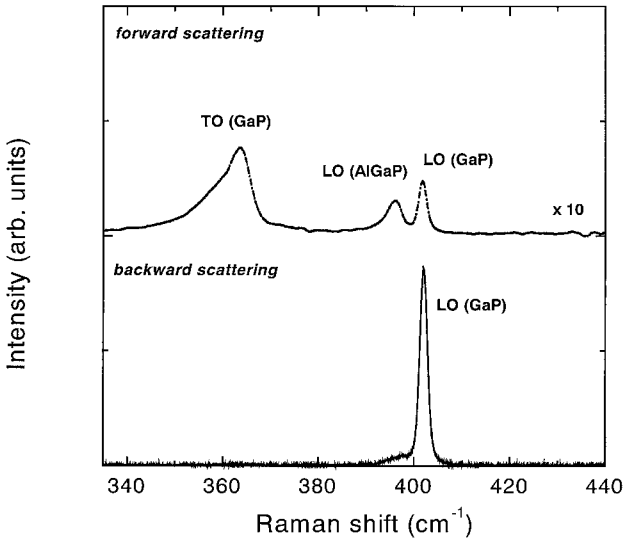

Fig. 6. Spontaneous Raman scattering spectra from a ⟨100⟩ directional waveguide for the forward scattering and backward scattering.

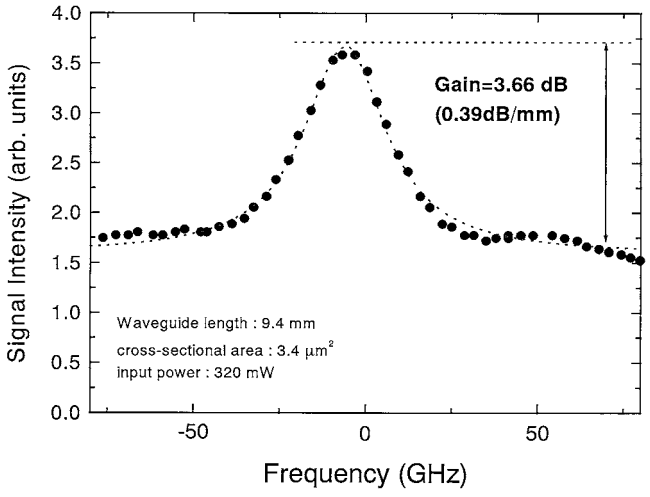

Fig. 7. Maximum Raman gain, which is obtained for a waveguide with the length of 9.4 mm, and the cross sectional area of 3.4 μm^2.

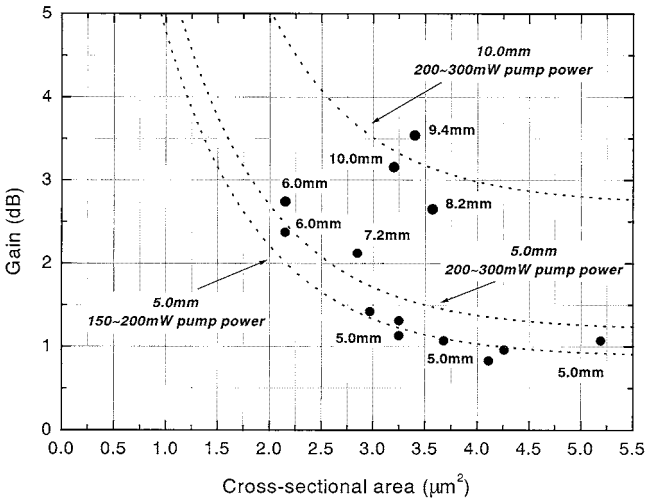

Fig. 8. The Raman gains of various waveguides versus the waveguide cross sectional areas and lengths.

about 16%/cm, i.e., 0.76 dB/cm, at least up to the waveguide length of 10 mm. In terms of the effective absorption coefficient, it is given as $\alpha_{\text{eff}} = 0.17$ cm^{-1}. This fact means that the waveguide length longer than 10 mm has become practical, although this value of α_{eff} is yet larger than a possible minimum loss due to free carrier absorption.

Before the amplification experiment, the spectral characteristics of the spontaneous Raman scattering from a waveguide has been measured for both the forward and backward scatterings. In this measurement, both the front and back facets of a waveguide are antireflection-coated. As is compared in Fig. 6, the observed spontaneous Raman spectrum is mainly composed of the LO phonon mode for the backward Raman scattering, while the transverse optical (TO) phonon mode is dominant for the forward Raman scattering. It should be noted that, for the forward scattering in a narrow waveguide with micrometer size, the wave momentum of phonons in the transverse directions becomes much larger than the wave momentum along the waveguide direction. This causes the change from the LO mode to the TO mode for the forward Raman scattering [12], [13].

Then, after the input facet is AR coated and the back facet is high-reflection coated, the amplification experiment is performed. The difference of the pump and signal light frequencies is set near the LO phonon frequency, 12.12 THz, by selecting the Ti-sapphire laser wavelength of 824 nm. The wavelength of the DBR laser diode for the signal light is approximately fixed at 853 nm, but can be swept over 300 GHz by changing the Peltier-controller temperature. From the spontaneous Raman scattering experiment, it is understood that the backward Raman scattering mainly contributes to the Raman amplification. Therefore, the signal light propagating in the forward direction interacts with the pump light reflecting back from the back reflector and vice versa.

Fig. 7 shows the gain spectrum around the LO phonon frequency shift for the best stripe with the length of 9.4 mm. The spectrum is obtained with sweeping the DBR laser diode frequency. The waveguide cross section is $\sigma = 3.4$ μm^2 ($w = 2.8$ μm, and $d = 1.2$ μm). The maximum amplifier gain is found to be 3.7 dB at a CW pump power level of 320 mW.

Fig. 8 compares amplifier gains for various waveguides with different lengths and different cross sections. The maximum gain per waveguide length is 4.6 dB/cm, which is obtained for a waveguide with length of 6.0 mm and a cross section of 2.15 μm^2. From these results, we can expect a further improvement in gain. For example, for a waveguide with $l = 15$ mm and $\sigma = 2.2$ μm^2, an amplifier gain of 7 dB can be expected, if the low-loss nature is maintained.

Next, we describe the amplifier characteristics under pulse pumping. Compared to the CW pumping, pulse pumping has the merit of acting as a time gate function. Only a selected pulse channel can be amplified for each of the wavelength channels. Also, a higher Raman gain is available for pulse pumping. The experiment has been performed using a mode-locked Ti–sapphire laser. As a signal wave source, wavelength-tunable CW laser diode has been used. The pump and signal wavelengths are approximately 925 and 960 nm, respectively. The pump

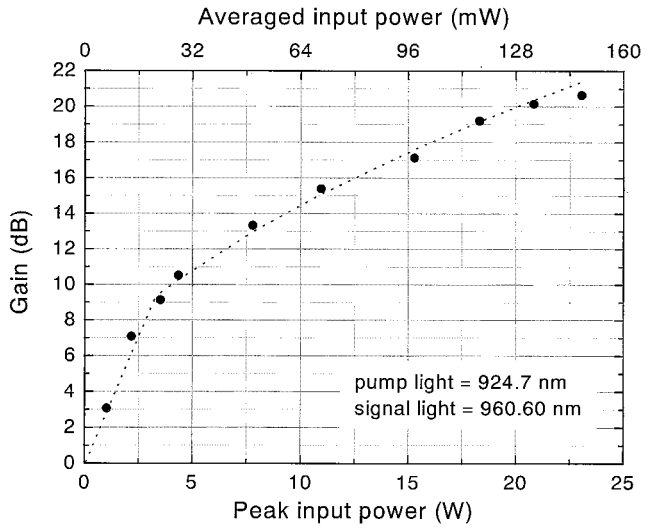

Fig. 9. Raman gain for pumping with 80-ps pulses. The length and the cross-sectional area of the waveguide are 2.7 μm^2 and 7.2 mm, respectively.

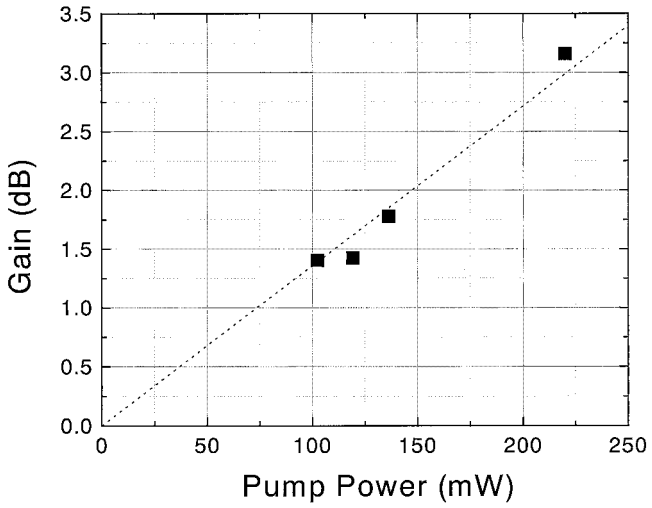

Fig. 10. Raman gain versus CW pump power for a waveguide with a length of 10 mm and a cross-sectional area of 5 μm^2.

pulsewidth measured by the autocorrelation method is 80 ps, and the pulse repetition rate is 80 MHz. It takes about 150 ps for a round trip of a light wave in a 7.2-mm-long GaP–AlGaP waveguide. Therefore, the pulsewidth is shorter than the round-trip time in the waveguide.

Fig. 9 shows the result of Raman gain measurement. The observed maximum gain is 20 dB at an average pump power of 150 mW. This power corresponds to a pulse peak power of 25 W. The Raman gain in decibel units shows a linear dependence at a low pump power level, but becomes nearly proportional to the square root of the peak pump power at a higher gain exceeding 10 dB. It should be noted that 10-dB amplification can be obtained with an average pump power as low as 25 mW.

When the maximum gain is 20 dB, the FWHM of the gain band is measured to be about 20 GHz. On the other hand, the FWHM of the Raman gain coefficient g was found to be 24 GHz in our earlier experiment [11], [12]. The amplifier gain G is described as $G = \exp(2gI_p l)$. The value of g and its FWHM was determined by a gain measurement at a low pump power level. From the FWHM of g, we can expect that the FWHM of the amplifier gain at a level of 20 dB is 10.1 GHz. That is, the measured value is two times larger than the expected one. Therefore, it is thought that the observed gain bandwidth is broadened due to the spectral bandwidth of the mode-locked pump light. When the spectral bandwidth of the pump light is larger than that of the gain expected for a single frequency pumping, an amplifier gain is expected to be nearly proportional to the square root of the peak power of pump light. Although a more detailed analysis will be described elsewhere, the sublinear behavior in Fig. 9 can be interpreted to be the effect of the finite line width of the pump light due to the mode locking.

The pump power dependence of the Raman gain may be affected by nonlinear absorption. We reported that the nonlinear absorption in GaP waveguides occurs at wavelength shorter than 900 nm and nearly linearly increases with decreasing the wavelength [11]. It should be noted that much stronger nonlinear absorption has been observed in InP waveguides [18]. In the present experiment, the pulse pumping experiment has been performed at a pump wavelength of 924 nm, which is longer than the two-photon absorption edge, so that gain saturation against pump power due to the nonlinear absorption is not expected. Actually, in our earlier experiment using a 1.06-μm YAG laser pump source with a pulsewidth of 60 ns, which is long enough compared to the bandwidth of the gain coefficient, linear dependence was confirmed up to a gain of 10 dB [19].

In contrast, the present CW-pumping experiment has been performed at a pump wavelength of 824 nm, at which small nonlinear absorption is expected. Therefore, we have confirmed the linearity of the CW gain against pump power for one of the devices, as shown in Fig. 10. As a result, there is no apparent evidence of the CW gain saturation that should be caused by the nonlinear absorption, within a present level of CW pump power.

IV. Discussion and Conclusion

The semiconductor Raman amplifier will be useful for selecting one desired wavelength channel from many channels extending over terahertz bandwidth, with each subscriber connected by optical fiber network, rather than for demodulating all of the channels in the main line. For this purpose, the pump source must be wavelength tunable. A laser diode, as a possible pump source, can be wavelength tuned via current [20] or temperature [21], or by using a grating. In any case, the CW Raman gain should be made higher. It is noted that the Raman gain in decibel units, G(dB), is proportional to the pump power density and the waveguide length. Therefore, it is important to further reduce the waveguide cross-sectional dimensions and increase the waveguide length, while keeping the minimum optical loss. It is noted that tapered waveguide structure will be effective to increase the pump power density [8].

The time gate function will be desired because one wavelength channel should contain hundreds of pulse channels and each subscriber needs to select one from them. In the present experiment, the pump pulsewidth is 80 ps, which is near to that

limited by the gain bandwidth of the GaP waveguide. The pulse repetition frequency is 80 MHz, which is thought to be enough high because the experiment corresponds to selection of one channel with 80 Mb/s from 152 pulse channels within one wavelength channel having a capacity of 10 to 25 GHz bandwidth. Changing pulse channel from one to another can be made by the phase change of mode locking of the pump laser. We note that there is a possibility of using a mode-locked laser diode with wavelength tunable external cavity structure as a pump source with suitable repetition rate, pulsewidth, and peak intensity enough to obtain high gain exceeding 20 dB [22].

It should be noted that the Raman gain coefficient is expected to be proportional to the signal light frequency [23]. Therefore, at a signal light wavelength of 1.5 μm, the Raman gain in decibel units is thought to reduce by a factor of about 2/3. However, optical loss due to deep levels will also reduce.

In conclusion, GaP–AlGaP waveguide structure Raman amplifier with micrometer size narrow stripe and the length up to 10 mm are investigated. As a result of reduced optical loss, the CW Raman gain of 3.7 dB has been obtained. Also, the time-gated amplification with 80-ps pulse pumping is performed and 20-dB gain is obtained. Such performances are useful in frequency selection using the semiconductor Raman amplifier in terahertz bandwidth and WDM optical communication systems.

REFERENCES

[1] J. Nishizawa, "History and characteristics of semiconductor laser," *Denshikagaku*, vol. 14, pp. 17–20, 1963.

[2] J. Nishizawa and K. Suto, "Semiconductor Raman laser," *J. Appl. Phys.*, vol. 51, pp. 2429–2431, 1980.

[3] B. A. Weinstein and M. Cardona, "Resonant first- and second order Raman scattering in GaP," *Phys. Rev.*, vol. B8, pp. 2795–2809, 1973.

[4] G. Kh. Bairamov, "Scattering of light by coupled plasmon-phonon oscillations in p-GaP and lifetime of optical phonons with $k = 0$ in insulating GaP," *Sov. Phys. Solid State*, vol. 19, pp. 261–265, 1977.

[5] R. H. Stolen, E. P. Ippen, and A. R. Tynes, "Raman oscillation in glass optical waveguides," *Appl. Phys. Letters*, vol. 20, pp. 62–64, 1972.

[6] J. M. Yarborough, S. S. Sassman, H. E. Puthoff, R. H. Pantel, and B. C. Johnson, "Efficient tunable optical emission from $LiNbO_3$ without a resonator," *Appl. Phys. Letters*, vol. 15, pp. 102–105, 1969.

[7] K. Suto, S. Ogasawara, T. Kimura, and J. Nishizawa, "Buried heterostructure semiconductor Raman laser with threshold pump power less than 1W," *J. Appl. Phys.*, vol. 66, pp. 5151–5155, 1989.

[8] K. Suto, T. Kimura, and J. Nishizawa, "Fabrication and characteristics of tapered waveguide semiconductor Raman lasers," *Inst. Elec. Eng. Proc. Optoelectron.*, vol. 143, pp. 113–118, 1996.

[9] K. Suto, T. Kimura, T. Saito, A. Watanabe, and J. Nishizawa, "GaP $Al_xGa_{1-x}P$ waveguide Raman lasers and amplifiers for optical communication," in *Proc. 24th IEEE Int. Symp. Compound Semiconductors*, San Diego, CA, Sept. 8–11, 1997, pp. 573–576.

[10] K. Suto, T. Kimura, and T. Saito, "Output power saturation characteristics of the CW-operated semiconductor Raman laser," *Inst. Elec. Eng. Proc. Optoelectron.*, vol. 145, pp. 243–247, 1998.

[11] K. Suto, T. Kimura, T. Saito, and J. Nishizawa, "Raman amplification in GaP $Al_xGa_{1-x}P$ waveguides for light frequency discrimination," *Inst. Elec. Eng. Proc. Optoelectron.*, vol. 145, pp. 105–108, 1998.

[12] T. Saito, K. Suto, T. Kimura, A. Watanabe, and J. Nishizawa, "Raman gain and optical loss in GaP–AlGaP waveguides," *J Appl. Phys.*, vol. 87, pp. 3399–3403, 2000.

[13] T. Saito, K. Suto, J. Nishizawa, and M. Kawasaki, "Spontaneous Raman scattering in [100], [110], and [11-2] directional GaP waveguides," *J. Appl. Phys.*, 2001.

[14] J. Nishizawa and Y. Okuno, "Liquid phase epitaxial growth of GaP by a temperature difference method under controlled vapor pressure," *IEEE Trans. Electron Devices*, vol. ED-22, pp. 716–719, 1975.

[15] K. Suto, T. Kimura, S. Ogasawara, and J. Nishizawa, "Heteroepitaxy of GaP–$Al_xGa_{1-x}P$ system by the temperature difference method under controlled vapor pressure (TDM-CVP)," *J. Cryst. Growth*, vol. 99, pp. 297–301, 1990.

[16] T. Saito, Y. Oyama, K. Suto, J. Nishizawa, and T. Kimura, "Excess ion density at the GaP/AlGaP liquid-phase epitaxial regrowth interface," *J. Cryst. Growth*, vol. 209, pp. 666–674, 2000.

[17] T. J. Yu, K. Suto, and J. Nishizawa, "Investigation of deep levels in GaP liquid phase epitaxial layers on substrates with vapor pressure heat treatment," in *Proc. Material Research Society Symp.*, vol. 588, 1999, pp. 61–66.

[18] D. Van Thourhout, C. R. Doerr, C. H. Joiner, and J. L. Pleumeekers, "Observation of WDM crosstalk in passive semiconductor waveguides," *IEEE Photon. Technol. Lett.*, vol. 13, pp. 457–459, May 2001.

[19] T. Saito, K. Suto, T. Kimura, and J. Nishizawa, "Gain of high-intensity pulse-pumped GaP–AlGaP waveguide Raman amplifier," *IEE Proc. Optoelctron.*, vol. 146, pp. 209–212, 1999.

[20] G. M. Smith, J. S. Hughes, R. M. Rammert, M. L. Osowski, G. C. Papen, J. T. Verdeyen, and J. J. Coleman, "Wavelength-tunable asymmetric cladding ridge-waveguide distributed Bragg reflector lasers with very narrow linewidth," *IEEE J. Quantum Electron.*, vol. 32, pp. 1225–1229, July 1996.

[21] S. Sakano, T. Tsuchiya, M. Suzuki, S. Kitajima, and N. Chinone, "Tunable DFB laser with a striped thin film heater," *IEEE Photon. Technol. Lett.*, vol. 4, pp. 321–322, Apr. 1992.

[22] L. Goldberg, D. Mehuys, and D. Welch, "High power mode-locked compound laser using a tapered semiconductor amplifier," *IEEE Photon. Technol. Lett.*, vol. 6, pp. 1070–1072, Sept. 1994.

[23] K. Suto and J. Nishizawa, *Semiconductor Raman Lasers*. Norwood, MA: Artech House, 1994.

Ken Suto (M'74) was born in Urawa City, Japan, on June 23, 1940. He received the B.S., M.S., and Doctor of Engineering degrees from the University of Tokyo, Tokyo, Japan, in 1963, 1965, and 1968, respectively.

In 1968, he became a Research Assistant at the Research Institute of Electrical Communication, Tohoku University, Sendai, Japan, becoming an Associate Professor in 1969. In 1991, he became a Professor in the Department of Materials Science, Faculty of Engineering, Tohoku University. His research has focused on optoelectronic semiconductor materials, especially stoichiometry control and liquid phase growth of compound semiconductors such as GaP, AlGaAs, HgCdTe, ZnSe, and PbTe. He has also studied optoelectronic devices, such as high-efficiency AlGaAs and GaP light emitting diodes, and semiconductor Raman lasers and Raman amplifiers.

Takao Saito (M'81) was born in Hiroshima City, Japan, on October 9, 1973. He received the B.S., M.S., and Ph.D. degrees in material science and engineering from Tohoku University, Sendai, Japan, in 1996, 1998, and 2001, respectively.

In 2001, he joined NGK Insulators, Ltd., Nagoya, Japan, where he works on the research and development of SI thyristors.

Tomoyuki Kimura was born in Miyagi, Japan, on November 22, 1965.

In 1984, he joined the Semiconductor Research Institute, Sendai, Japan, where he researches semiconductor Raman lasers and amplifiers.

Jun-Ichi Nishizawa (M'57–SM'62–F'69–LF'93) was born in Sendai, Japan, on September 12, 1926. He received the B.S. and Dr. Eng. degrees from Tohoku University, Sendai, Japan, in 1948 and 1960, respectively.

In 1954, following a year as a Research Assistant, he became an Associate Professor at Tohoku University, and was made a Professor in 1962. In 1968, he was appointed the Director of the Semiconductor Waste Institute, Sendai. From 1983 to 1986 and from 1989 to 1990, he was the Director of the Research Institute of Electrical Communication, Tohoku University. From 1990 to 1996, he was the President of Tohoku University. Currently, he is the President of Iwate Prefectrual University, Iwate, Japan. His main work has involved the invention of p-i-n diodes and p-n-i-p (n-p-i-n) transistors in cooperation with p-i-n photodiodes in 1950, avalache photodiodes in 1952, semiconductor injection lasers in 1957, solid-state focusing optical fibers in 1964, and transit-time effect negative-resistance diodes in 1954, including the avalanche and tunnel injections (1958), hyper abrupt variable capacitance diode (1959), semiconductor inductance (1957), and static induction transistor (1950 and 1971). Currently, he specializes in the development of static induction transistor to high-frequency and high-power devices, the high-speed thyristor, the high-speed and low-pwer dissipation integrated circuit, and the growth method of III–V compound semiconductors, a temperature difference method under controlled vapor pressure giving rise to high-efficiency light-emitting diodes and long-life diodes based on silicon perfect crystal technology by lattice constant compensation. He also originated electroepitaxy in 1955, photoepitaxy in 1961, and molecular-layer epitaxy in 1984. In 1953, he discovered the avalache effect in semiconductors and explained the backward character of the p-n junction by this effect.

Dr. Nishizawa is a member of the Japan Academy.

Tadao Tanabe was born in Sapporo City, Japan, on February 7, 1973. He received the M.S. and Doctor of Engineering degrees from Tohoku University, Sendai, Japan, in 1997 and 2000, respectively.

In 2000, he became a Researcher at Venture Business Laboratory, Tohoku University, and in 2001, he became a Research Associate in the Department of Materials Science, Graduate School of Engineering, Tohoku University. His research interests include optoelectronic semiconductor materials, particularly interface control, and optoelectronic devices such as Raman amplifiers.